



Adhesion control for Micro- and Nano-Manipulation.

Jérôme Dejeu, Mikhael Bechelany, Patrick Rougeot, Laëtitia Philippe,
Michaël Gauthier

► To cite this version:

Jérôme Dejeu, Mikhael Bechelany, Patrick Rougeot, Laëtitia Philippe, Michaël Gauthier. Adhesion control for Micro- and Nano-Manipulation.. ACS Nano, 2011, 5 (6), pp.4648-4657. 10.1021/nn200658z . hal-00604671

HAL Id: hal-00604671

<https://hal.science/hal-00604671>

Submitted on 29 Jun 2011

HAL is a multi-disciplinary open access archive for the deposit and dissemination of scientific research documents, whether they are published or not. The documents may come from teaching and research institutions in France or abroad, or from public or private research centers.

L'archive ouverte pluridisciplinaire **HAL**, est destinée au dépôt et à la diffusion de documents scientifiques de niveau recherche, publiés ou non, émanant des établissements d'enseignement et de recherche français ou étrangers, des laboratoires publics ou privés.

Adhesion Control for Micro- and Nano-Manipulation

Jérôme Dejeu,[†] Mikhael Bechelany,^{‡,§} Patrick Rougeot,[†] Laëtitia Philippe,[¶] and
Michaël Gauthier*,[†]

*FEMTO-ST Institute, UMR CNRS 6174 - UFC / ENSMM / UTBM, 24 rue Alain Savary, 25000
Besançon, France, Institut Européen des Membranes de Montpellier (IEMM, UMR CNRS 5635,
ENSCM), Place Eugène Bataillon, 34095 MONTPELLIER Cedex 5, France , and
EMPA-Materials Science & Technology, Laboratory for Mechanics of Materials and
Nanostructures, Feuerwerkerstrasse 39, CH-3602 Thun, Switzerland*

Abstract

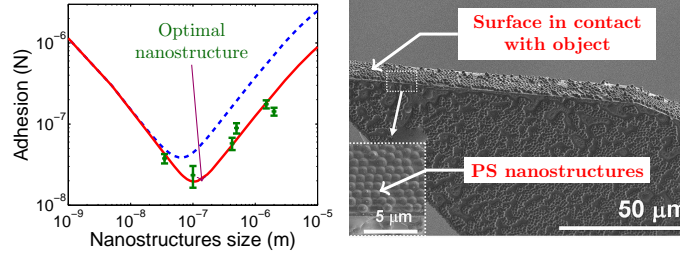
The adhesion between a micro/nano-object and a micro-gripper end-effector is an important problem in micromanipulation. Cancelling or reduction this force is a great challenge. This force is directly linked to the surface chemical structure of the object and the gripper. We propose to predict this force between a structuring surface and a micro-object with a multi-sphere van der Waals force model. The surface was structured by polystyrene latex particles (*PS* particles) with *radii* from 35 to 2000 *nm*. The model was compared with experimental pull-off force measurement performed by *AFM* with different natures of spheres materials glued on the tipless. A wide range of applications, in the field of telecommunications, bioengineering, and more generally speaking *MEMS* can be envisaged for these substrates.

[†]FEMTO-ST Institute

[‡]IEMM

[¶]EMPA

[§]Work done at: EMPA-Materials Science & Technology, Laboratory for Mechanics of Materials and Nanostructures, Feuerwerkerstrasse 39, CH-3602 Thun, Switzerland



Keywords: surface structuring, adhesion force, pull-off force, *PS* latex particle, micromanipulation, grippers, nanomanipulation.

Introduction

Manufactured products are getting smaller and smaller and are integrating more and more functionalities in small volumes. Several application fields are concerned such as bio-engineering, telecommunications or more generally speaking the Micro-Electro-Mechanical-Systems (*MEMS*). The assembly of these microproducts is a great challenge because of the microscopic size of the components.¹ In fact, the major difficulty of micro/nano-assembly comes from the particularity of the micro/nano-objects behaviour which depends on surface forces.²⁻⁴ The manipulation of a micro-object requires handling, positioning, and releasing it without disturbances of the surface forces such as electrostatic forces, van der Waals forces or capillary forces.

Current microhandling methods are able to improve micromanipulation but the object behaviour is always disturbed by adhesion and thus the repeatability and reliability is still low.^{5,6} The required force to separate two surfaces is commonly called the "pull-off" force. The "pull-in" force is the attractive force between two objects when they approach closely. The pull-off force is not well understood and must be studied further to enable the advent of reliable micromanipulation techniques. Current methods to measure micro/nanoforces between surfaces are the Surface Force Apparatus (*SFA*),^{7,8} the Atomic Force Microscope (*AFM*),⁹⁻¹¹ capacitive force sensors¹² or nanoindentation testers.^{13,14} The modeling of pull-off force is mainly based on two different approaches based on the surface energies on the contact,¹⁵⁻¹⁸ or on the integration of the van der

Waals forces between objects^{19–22} and on some hybrid approaches between both.^{23,24} The adhesion force reduction was already obtained in liquid and dry medium by surface structuring^{24–26} or chemical functionalisation.^{9,27–29} The last technique allows to switch the force from attractive to repulsive by pH solution modification and improves the micro-object manipulation.^{27,30,31} In case of randomly rough surfaces, fractal approach is one of the most usual way to predict wear, adhesion force or interaction forces.^{32–34}

Thanks to the surface structuring, we can reduce the contact area between the gripper and the objects, and in turn this will decrease the contact area and van der Waals forces. Also, we can induce specific properties of the gripper such as using electrically conductive materials to minimize electrostatic force. In practice, the approach for surface structuring can be categorized into two directions: top-down and bottom-up approaches. Top-down approaches encompass template-based techniques,³⁵ and plasma treatment of the surfaces.³⁶ Bottom-up approaches involve mostly self-assembly and self-organization³⁷ as for instance chemical deposition,³⁸ layer-by-layer (*LBL*) deposition,³⁹ and colloidal assemblies.⁴⁰ There are also methods based on the combination of both bottom-up and top-down approaches, for example, casting of polymer solution and phase separation,⁴¹ and electrospinning.⁴² Among these methods, the application using two-dimensional (*2D*) colloidal crystals, called "natural lithography", which has been suggested by Deckman and Dunsmuir,⁴³ has attracted attention due to it being a relatively easy process in comparison with conventional lithography technique.⁴³ Based on such a process, uniformly sized microstructures and nanostructures could be produced on a substrate using a mono or multilayer colloidal spheres. In recent years, various techniques, based on "nanosphere lithography", have been reported for nano/microfabrication or nano/micropatterning of a wide variety of solid substrates including metals,^{44–48} semiconductors^{49,50} and ceramics.⁵¹

Recently, we reported structuring surface by nanospheres lithography and measured the adhesion force. We have proposed a multisphere van der Waals force model which may suggest the existence of an optimal value of the sphere *radius* which minimizes the adhesion. In the case of

the $20\ \mu m$ borosilicate sphere diameter, the pull-off force is reduced to $20\ nN$ by the *PS* particles layer with a *radius* of $45\ nm$.²⁶ The aim of this paper is to extend this model and to demonstrate the existence of *minimum* dependently of the spheres diameter and nature. First, an improved model compared to our previous paper²⁶ is going to be proposed then the spheres parameters as diameter and nature are studied. The analysis of the correlation between the experimental measures and the model and a discussion on the application relevance in micromanipulation tasks are performed. The paper is concluded by the surface patterning method and the adhesion measurement methodology.

Model developed

Usually force measurements are conducted between a sphere and a planar substrate where the contact surface is necessary a unique surface. In our case, the substrate is structured with several microspheres and the contact numbers must be studied.

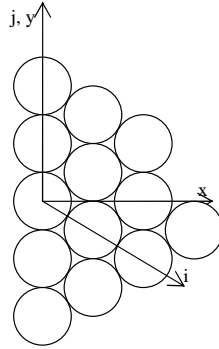


Figure 1: Arrangement of the *PS* spheres on the substrate.

Let us consider the arrangement described in Figure 1 which represents the position of the *PS* sphere on the substrate (noted S_b). In an application case and also during force measurements the location of the sphere on the probe up the structured surface cannot be controlled precisely. When the probe with a sphere, (noted S_a), is approaching, it touches the nanospheres r_2 (Figure 2) on a non-control position. Two extreme cases are considered:

- the probe r_1 is perfectly aligned with one sphere r_2 (e.g. the sphere $i=0, j=0$), it generates

only one contact point. This case induces the minimal force between the probe and the nanostructured surface;

- the probe r_1 is up to the centroid of three adjacent sphere r_2 (e.g. the sphere $i=0,j=0$; $i=0,j=1$; $i=1,j=1$); it generates three contact points which maximize the interaction force between the probe and the nanostructured surface.

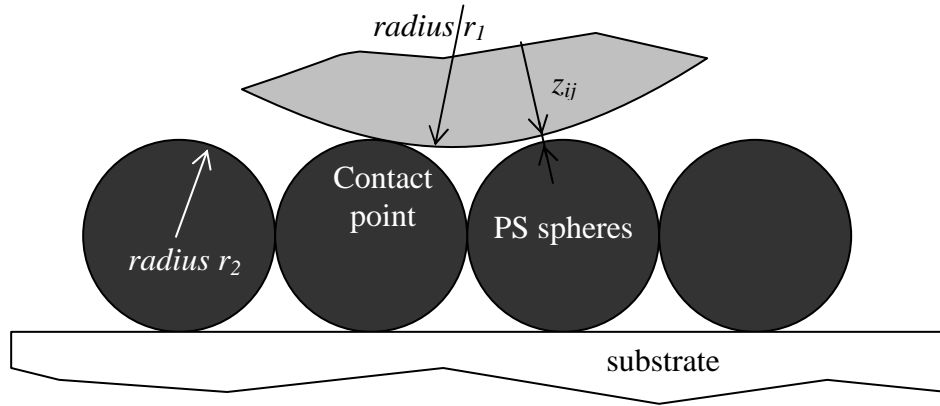


Figure 2: Description of the contact between the probe and the *PS* spheres on the substrate.

The objective of the model is to predict adhesion force between the nanostructured surface and the microsphere. One of the originality of our approach is the scale where the measurements are done linked with the microhandling application. The *radius* of the sphere r_1 is only $10\text{ }\mu\text{m}$ and the *radius* of the sphere r_2 are in the nanoscale. Consequently the equivalent *radius* equation (4) of the contact is usually below several micrometers.

In the microscale and in the nanoscale, it has been shown that mechanical deformation becomes negligible and that adhesion is reduced to the value of interaction force established in a non-deformable shape as explained by Alvo *et al.*²¹ Consequently in nanoscale, adhesion is usually computed using van der Waals equations in spite of mechanical models DMT or JKR approaches which are relevant for larger equivalent *radius*.

The modeling force must be done in the case of one or three contact points. Based on a geometrical analysis (Figure 1 and Figure 2), the distance z_{ij} between the probe (r_1) and a sphere

(i, j) is respectively equation (1) or (2) for one or three contact points:

$$z_{ij_{min}} = \sqrt{(r_2 + z_0 + r_1)^2 + 4r_2^2(j^2 - ij + i^2)} - r_1 - r_2 \quad (1)$$

$$z_{ij_{max}} = \sqrt{(r_2 + z_0 + r_1)^2 + 4r_2^2(j^2 - ij - i - j + i^2)} - r_1 - r_2 \quad (2)$$

Based on Alvo *et al.*,²¹ the impact of local deformation on the calculation of van der Waals force can be neglected in the nanoscale, thus we are considering the force between two rigid spheres. The van der Waals force z_{ij} between the probe and the sphere (i, j) verifies:

$$\|\vec{F}_{ij}\| = \frac{A_{12}r_{12}}{6z_{ij}^2}, \quad (3)$$

where r_{12} is the equivalent *radius* and A_{12} the Hamaker constant which can be calculated using the approximative combination law:

$$\frac{1}{r_{12}} = \frac{1}{r_1} + \frac{1}{r_2}, \quad (4)$$

$$A_{12} = \sqrt{A_1 \cdot A_2}, \quad (5)$$

where A_i is the Hamaker constant of the material i .

The total force F_{Tvdw} between an infinite plan structured with *PS* spheres and the probe is thus:

$$F_{Tvdw} = \sum_{i,j}^{\mathbb{Z}^2} \vec{F}_{ij} \cdot \vec{z} \quad (6)$$

The modeling force for one and three contacts zone can be obtained respectively by:

$$F_{Tvdw_{min}} = A_{12} \sum_{i,j}^{\mathbb{Z}^2} \frac{r_{12}}{6z_{ij_{min}}^2} \cdot \frac{r_2 + z_0 + r_1}{r_2 + z_{ij_{min}} + r_1} \quad (7)$$

$$F_{Tvdw_{max}} = A_{12} \sum_{i,j}^{\mathbb{Z}^2} \frac{r_{12}}{6z_{ij_{max}}^2} \cdot \frac{\sqrt{(r_2 + z_0 + r_1)^2 - (4/3 \cdot r_2^2)}}{r_2 + z_{ij_{max}} + r_1} \quad (8)$$

The equation of the pull-off force is function of materials used, through the approximative combination law of on Hamaker constant A_{12} , and of the spheres size through $\sum_{i,j}^{\mathbb{Z}^2} \frac{r_{12}}{6z_{ij_{max}}^2} \cdot \frac{\sqrt{(r_2 + z_0 + r_1)^2 - (4/3 \cdot r_2^2)}}{r_2 + z_{ij_{max}} + r_1}$. This model of the interaction between a spherical probe and a structured surface has been simulated using the Matlab Simulink software and is presented figure 3(a) for $12.5 \mu m$ PS spheres radius on the tipless cantilever *versus* the PS spheres radius on the substrate.

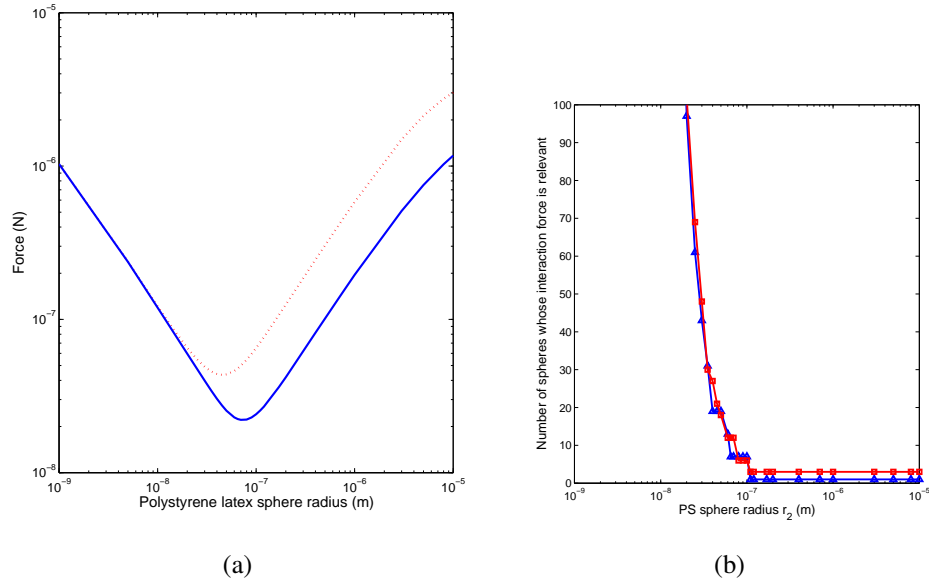


Figure 3: a) Adhesion force modeling (one contact point, blue solid line, and three contact points, red dash line) on the structuring PS surface for $12.5 \mu m$ PS sphere radius, r_1 , glued on the tipless ($z_0 = 0.25 \text{ nm}$); b) the PS spheres number influencing the adhesion force modeling (threshold 5 %) *versus* the PS sphere radius on the structuring surface for one (\triangle) and (\square) three contact point.

Figure 3(a) shows the presence of a *minimum* interaction force which represents an *optimum* of adhesion reduction in the applicative field of micromanipulation. This *minimum* is weakly dependent of the contact number. There is 30 nm and 20 nN between the two optima. The second observation is the influence of the initial contact number on the pull-off force and the third is the

force increasing after the optimal *radius*. Indeed, to explain that, it is necessary to determine the number of *PS* spheres whose interaction force is relevant (figure 3(b)). In this case, we consider that the spheres, around the contact point, are a relevant rule on the interactions when they increase the adhesion force of 5 %. At the beginning, for *PS radius* inferior to 10^{-7} m the neighbouring spheres of the contact point do not influence the adhesion force and this last are three times more important for the three contact points. After this *radius*, the spheres close to the contact point modify the pull-off force but with a weaker influence than the sphere at the initial contact point. Figure 3(a), the adhesion force are the same whatever the number of initial contacts for a *PS* sphere *radius* near to 10 nm. With the figure 3(b), we can deduce that 100 spheres around the contact point are necessary to obtain the same pull-off force.

Results

The model exposed previously must be validated by the experimental measurements. For that, structuring surfaces, with different *PS* sphere *radius* must be performed and were presented below. Then, the adhesion force was measured with an *AFM*, where a sphere is glued on the tipless cantilever extremity, *versus* the sphere properties: *radius* (between 35 nm and 2 μ m) and nature (borosilicate or carbon). The experimental adhesion forces measured were compared with the previous model. This model can not be correlated with the sphere mechanical deformation at the moment of the contact between the structuring surface and the cantilever. Indeed, this deformation can not be evaluated and observed because of the sphere size deposited on the surface.

Surface structuring

Layers of polystyrene *PS* spheres were created by spin coating *PS* spheres *radius* from 35 nm to 2150 nm (Figure 4) onto a *Si/SiO₂* substrates. The heating of the structured surface was necessary

in order to adhere the particle to the substrate. Indeed, without this step, it is impossible to scan the sample with particles because they moved along the surface.

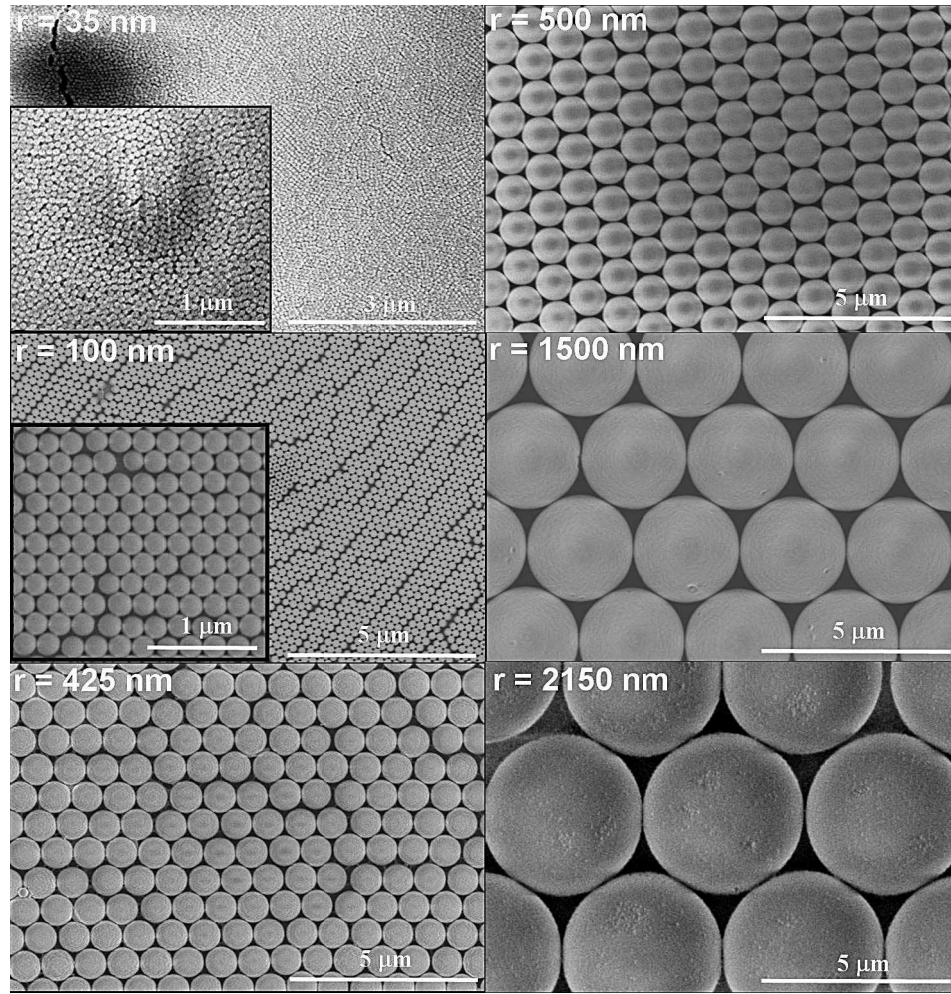


Figure 4: SEM images of a self assembled monolayer of PS spheres with a radius of a) 35 nm, b) 100 nm, c) 425 nm, d) 500 nm, e) 1500 nm and f) 2150 nm.

The layer created is a monolayer. The specimens were successfully coated with large domains of defect-free packing over the entire substrate surface. In Figure 4, the spheres arranged themselves into a close-packed structure of two-dimensional ordered lattices due to attractive capillary forces.

Force measurement

Six different $radii$ r_2 of PS sphere structuring on silicon wafer have been tested with different borosilicate and carbon spheres r_1 , glued on S_a tipless cantilever and measured by SEM . Fifteen measurements were performed in different locations on the sample.

Influence of the PS sphere size

The force distance measurements obtained, with borosilicate sphere diameter of $20\ \mu m$, for different structured surfaces are presented in Figure 5 and are discussed below.

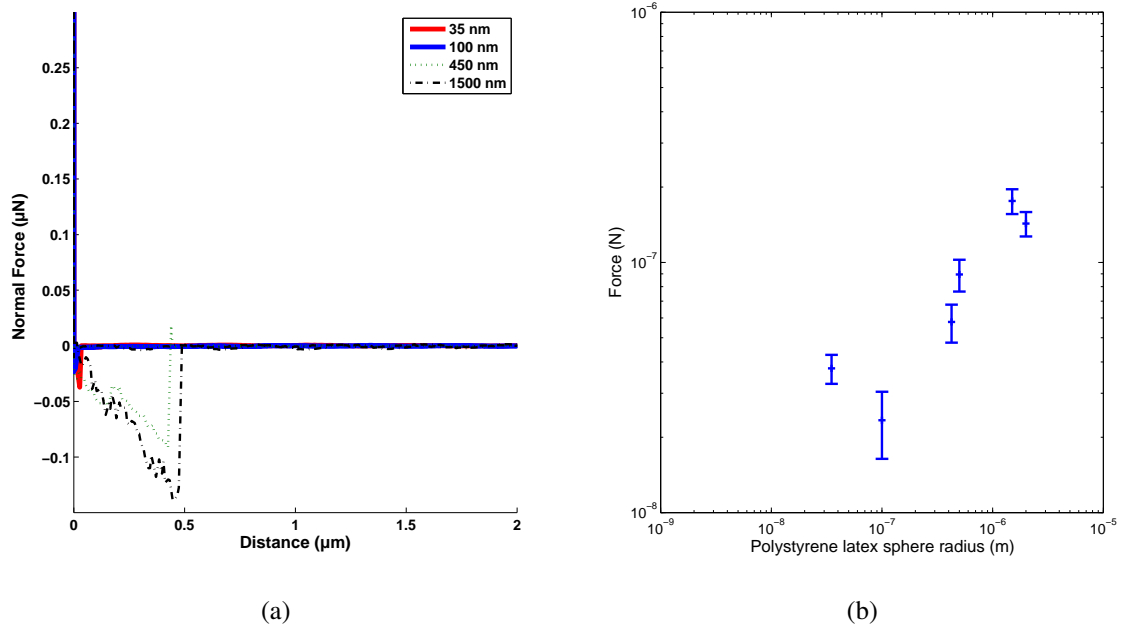


Figure 5: a) Force-distance curves, for a structuring surface by different PS latex particles sizes with a $radius$ of $35\ nm$ (red line), $100\ nm$ (blue line), $450\ nm$ (--- green) and $1.5\ \mu m$ (--- black); b) the summarize of the measurements. Stiffness: $0.3\ N/m$ and borosilicate $radius$: $20\ \mu m$.

In Figure 5, the size of the PS latex particles has an important influence on the adhesion. Indeed, decreasing the size from $2000\ nm$ to a value spread from 35 and $100\ nm$ reduces the adhesion force nearly 10 times. After this value, the adhesion force increases. This shows the existence of an optimal value of the nanostructure $radius$ r_2 , which is going to be explained using the model.

Influence of the borosilicate sphere size

Figure 6 presents the pull-off force measured between a structured surface with the *PS radius* r_2 100 nm and different borosilicate spheres whose *radius* r_1 is from 5 to 50 μm .

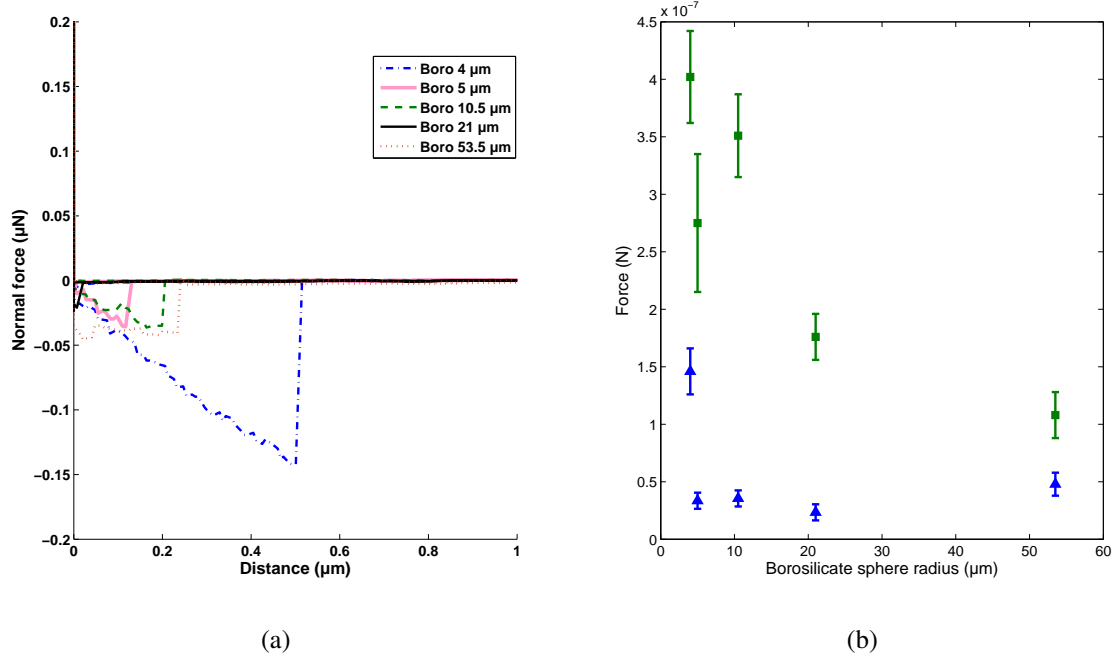


Figure 6: a) Force-distance curves, for a structuring surface with 100 nm *PS* latex spheres and different borosilicate sphere sizes glued on the tipless: 4 μm (– – blue), 5 μm (pink line), 10.5 μm (– – green), 21 μm (black line), 53.5 μm (– – brown); b) the summarize of the measurements with all the borosilicate spheres and *PS radius* 100 nm (\blacktriangle) and 1500 nm (\blacksquare). Stiffness: 0.3 N/m.

In figure 6(a) and figure 6(b), the size of the borosilicate sphere S_a influences the pull-off measurements.

Influence of the material nature

To validate the model with different material natures, the pull-off force measurements were performed on a carbon sphere. Figure 7(a) presents the results of the measurement with a carbon sphere (*radius* 10 μm) on the structured surface and figure 7(b) compares the results between the borosilicate and the carbon sphere.

In Figure 7(b), the sphere composition S_a influences the value of the pull-off force. The adhe-

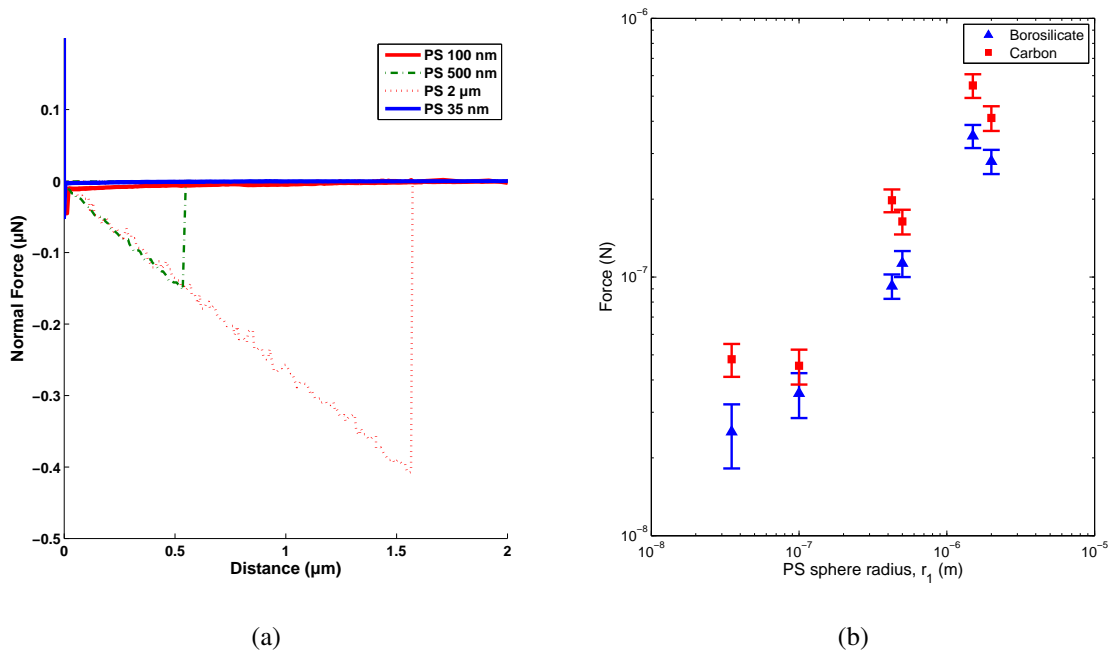


Figure 7: a) Force-distance curves, for a structured surface by different *PS* latex particles sizes with a *radius* of 35 *nm* (blue line), 100 *nm* (red line), 500 *nm* (– – green) and 2 μm (· · red); b) Comparison of the measurements between borosilicate and carbon sphere. Stiffness: 0.3 *N/m* and borosilicate (\blacktriangle) and carbon (\blacksquare) *radius* respectively 10.5 and 9 μm .

sion is greater for carbon sphere than borosilicate sphere. This phenomenon is correlated with the Hamaker constant. Indeed, it is $A_2 = 500 \text{ zJ}^{52}$ and $A_2 = 65 \text{ zJ}^{21}$ for respectively the carbon and the borosilicate sphere. The van der Waals force (3) based on the combination law, equation (5), increases with the Hamaker constant.

Model and experimental measurements comparison

The model exposed previously are compared with the experimental points on Figure 8. The Hamaker constant is respectively $A_{12} = 80 \text{ zJ}$ and $A_{12} = 180 \text{ zJ}$ for *PS*-borosilicate and *PS*-carbon and are imposed constant for all measurements on the same system. Only the parameter z_0 , contact distance, are modified with the diameter of the sphere glued on the tipless extremity. The value range is between 0.15 nm and 0.4 nm . The model of the interaction between a spherical probe and a structured surface has been simulated using the *Matlab Simulink software*.

The experimental point with borosilicate sphere S_a radius $50 \text{ }\mu\text{m}$ are not shown. Indeed the borosilicate sphere diameter is widely bigger than the cantilever breadth (respectively 100 and $45 \text{ }\mu\text{m}$). So the results obtained with this cantilever can be not assured and are not presented here.

The comparison between value predicted by the model and the measurement, plotted in Figure 8, shows a good concordance. So 90% of the experimental points validate the model. The other 10% of the experimental points are very near to the predicted value, just few $n\text{N}$ below the model. The majority of experimental points are on the force modeling with one contact point. The assumption of not taken into account the deformation can only underpredict the force in the model. As the measurements lie on the low end of the predicted adhesion, it seems to validate our assumptions and to show that deformation is negligible at this scale as predicted by Alvo *et al.*.²¹

It is impossible to predict in advance the number of contact between the probe and the structuring surface because it is impossible to image this contact. Indeed, the small size of the *PS* spheres needs *SEM* observations, the contact must be observed with a lateral view and there is no *SEM* with lateral view. Furthermore, the *PS* deposited planarity is not perfect and the sphere probe is

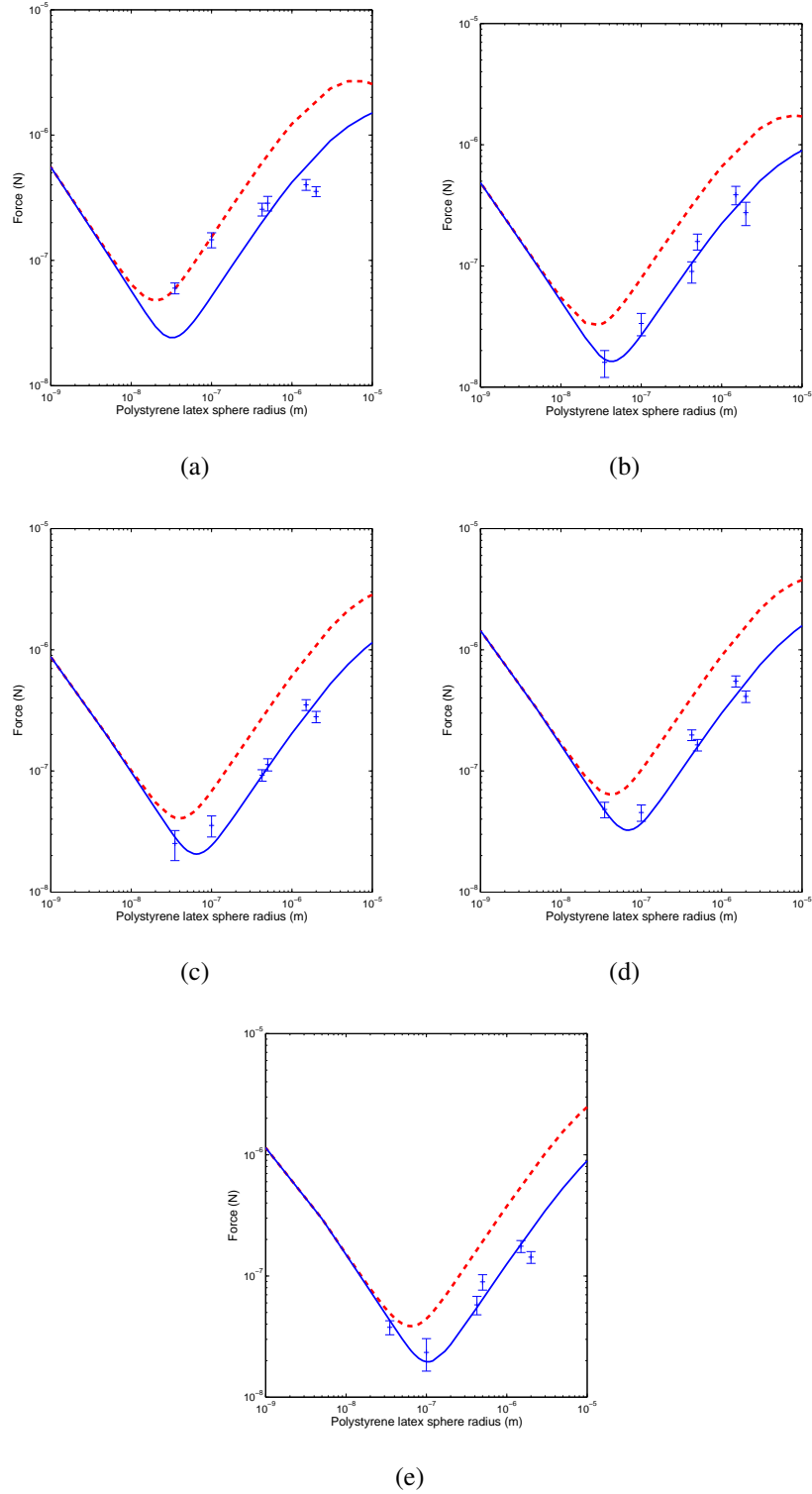


Figure 8: Comparison between the model (one contact point, blue solid line, and three contact points, red dash line) and experimental measurements (error bar) on the structuring surface for different sphere *radius*, r_1 , glued on the tiplless: a) borosilicate $4\ \mu\text{m}$ ($z_0 = 0.15\ \text{nm}$), b) borosilicate $5\ \mu\text{m}$ ($z_0 = 0.21\ \text{nm}$), c) borosilicate $10\ \mu\text{m}$ ($z_0 = 0.23\ \text{nm}$), d) carbon $9\ \mu\text{m}$ ($z_0 = 0.30\ \text{nm}$) and e) borosilicate $20\ \mu\text{m}$ ($z_0 = 0.30\ \text{nm}$).

bigger than the *PS* deposit create a shadowing area who obstructs the contact imaging. Moreover *SEM* observations are performed under vacuum. These conditions are not adapted to our controlled environment (humidity 30%).

The adhesion force obtained with the structuring surface are below than plan silicon substrate where the adhesion is near $1 \mu N$. Indeed, with the structured surface, the minimal force is near $10 nN$ and are decreasing 100 times. In our experimental case, the *optimum radius* r_2 in order to minimize the adhesion is between 35 and 70 *nm*. This value depends of the diameter of borosilicate sphere glued to the cantilever. For object manipulation where the size is known, a small variation of the *PS* sphere *radius*, deposited on the gripper and near of the minimal pull-off force, do not modify drastically adhesion force.

Discussion

The proposed model can be used to determine the diameter of the optimal particles spheres to be placed on a gripper to minimize adhesion force with a grasped sphere S_a . The model is useful whatever the manipulated objects and deposited spheres material nature.

The decreasing pull-off force ($f(r_1, r_2, z_0)$, equation(12)) obtained, after surface structuring against the plan surface ($F_{vdw_{plan}}$, equation (11)), can be evaluated from equation (7) or (8). In the follow, and with the observation done on the Figure 8, only the equation (7) modification are exposed:

$$F_{Tvdw_{min}} = \frac{A_{12}r_1}{6z_0^2} \cdot \frac{r_{12}}{r_1} \sum_{i,j}^{\mathbb{Z}^2} \frac{z_0^2}{z_{ij_{min}}^2} \cdot \frac{r_2 + z_0 + r_1}{r_2 + z_{ij_{min}} + r_1} \quad (9)$$

$$F_{Tvdw_{min}} = F_{vdw_{plan}} \cdot f(r_1, r_2, z_0) \quad (10)$$

where:

$$F_{vdw_{plan}} = \frac{A_{12}r_1}{6z_0^2} \quad (11)$$

$$f(r_1, r_2, z_0) = \frac{r_{12}}{r_1} \cdot \sum_{i,j}^{\mathbb{Z}^2} \frac{z_0^2}{z_{ij_{min}}^2} \cdot \frac{r_2 + z_0 + r_1}{r_2 + z_{ij_{min}} + r_1} \quad (12)$$

If the experimenter know the manipulated object size, he can determine the pull-off force decreasing if the spheres *radius* on the structured surface is imposed (figure 9(a)) or adapted the structured surface to optimize the pull-off force decreasing (figure 9(b)) with the abacus curve.

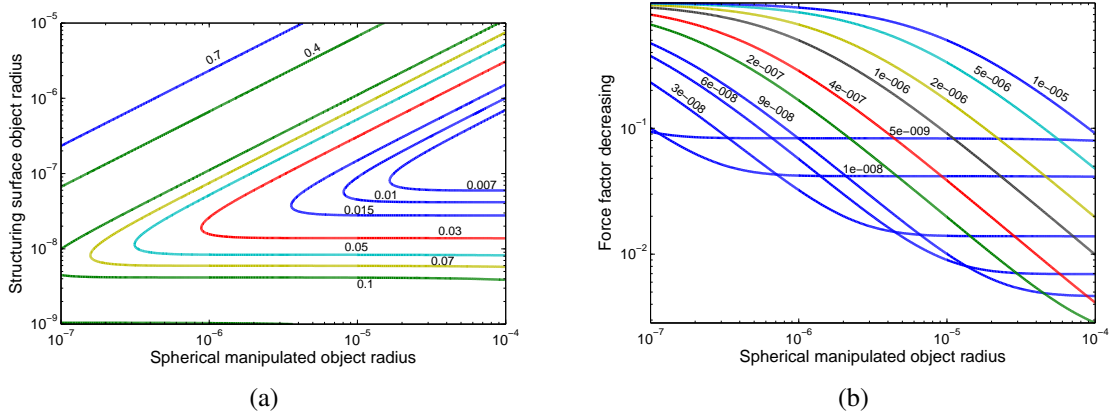


Figure 9: Abacus force for borosilicate probe sphere to a) determine the pull-off force decreasing or b) optimize the structured surface. The structure is *PS* spheres in our case.

With the Figure 9 and the equation (9), the researchers can control the pull-off force *via* changes the nature and the size of the material in a predictable manner.

Experimentally, some *PS* spheres have been deposited on silicon grippers⁵³ (see in Figure 10).

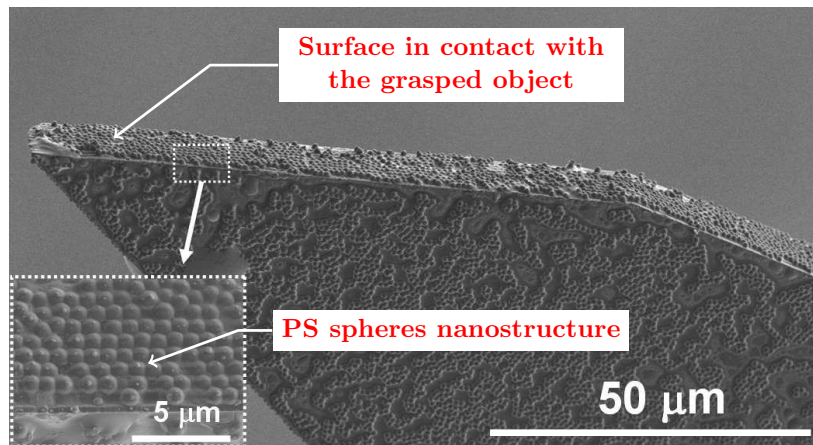


Figure 10: Structuring gripper by *PS* particles of 1 μm .

SEM images shows that *PS* spheres self-assembled into colloidal crystals which were close-packed structure with three-dimensional ordered lattices *via* attractive capillary force on *Si* grippers. These preliminary experiments show the feasibility of using natural lithography for patterning non planar complex *Si* grippers' tools with an extremely straightforward and simple method. More experiments are in progress in order to use these structured grippers for micro- and nanomanipulation.

Conclusion

In this paper, we have studied the interaction behavior, and most precisely the adhesion force, between a structured surface and carbon or borosilicate spheres. The experiments were performed as a function of the polystyrene latex particle *radii* from 35 to 2000 *nm* deposited on the silica substrate, and of *radii* and nature of the sphere glued on the tipless extremity. The experimental measurements were compared to a multisphere van der Waals model and show a good agreement. For a fixed sphere, the pull-off force decreases with the *PS radius* until a fixed value before to increase. The *PS radius* values for the minimal pull-off force are function of the sphere *radius* glued on the tipless cantilever, varied from 40 *nm* to 100 *nm* in our conditions.

Because adhesion is the current highest disturbance in micromanipulation (positioning and releasing), structured surface is a promising way to improve micro-object manipulation in the future. With the model presented, the size of the polystyrene spheres deposited can be optimized in function of the manipulated object material size and nature. This paper provides design rules to structure gripper surface in order to minimize adhesion. A wide range of applications, in the field of telecommunications, bioengineering, and more generally speaking *MEMS* can be also envisaged for these structured micro-grippers.

Materials and Methods

Surface structuring

Different sizes (*radius*, r_2 , between 35 nm and 2 μm) of commercially available *PS* microsphere (noted S_b) suspension were used (Polysciences, Inc., Eppelheim, Germany) as received. Acetone, H_2SO_4 (25%) and H_2O_2 (30%) were purchased from Aldrich and p-type Si wafers (5-10 $\Omega\cdot\text{cm}$, (111) crystal orientation) of dimensions 1.5 cm^2 from Silicon Materials were used as substrates. The deposit method was presented in the previous paper.²⁶ The different parameters of the spin coating were detailed in Table 1.

Table 1: Spin coating parameters *versus* the *PS* particles *radius*.

r_2	step 1	step 2
35 nm	300 rpm/10 s	2000 rpm/30 s
100 nm	300 rpm/10 s	1000 rpm/30 s
425 nm	300 rpm/10 s	1000 rpm/30 s
500 nm	300 rpm/10 s	500 rpm/30 s
1500 nm	300 rpm/10 s	400 rpm/30 s
2150 nm	200 rpm/10 s	300 rpm/30 s

After spin coating, the *PS* spheres organised on the *Si* substrate were characterised by Scanning Electron Microscopy (*SEM*, Hitachi, S-4800).

Grippers structuring

Si microgrippers⁵³ were pre-cleaned in acetone for 5 min and 1 wt % hydrofluoric acid (*HF*) for 5 min to remove organic contamination and native oxide on their surface. Then, pre-cleaned *Si* grippers were immersed in $\text{H}_2\text{SO}_4/\text{H}_2\text{O}_2$ (1/1) solution overnight to achieve hydrophilic surface. The gripper was dropped in a monodisperse suspension of polystyrene (*PS*) microspheres (1 μm in diameter) and dried in air overnight. The grippers were characterized by scanning electron microscopy (*SEM*, Hitachi, S-4800).

Force distance measurement by Atomic Force Microscopy

Characterisation of the pull-off force was performed with a commercial atomic force microscope (stand-alone *SMENA* scanning probe microscope *NT-MDT*). The experiments were done under a controlled environment with a laminar flow (humidity 30 % and 25 °C) on the Nanorol platform station. The "Nanorol platform" can be used by external person (<http://nanorol.cnrs.fr/events.php>). The rectangular silicon *AFM* cantilever, whose stiffness is 0.3 N/m, was fixed and the substrate moved vertically. The same kind of cantilever was used for all experiments. As the objective of this work is to improve the reliability of micro-object manipulation, interactions have been studied between a micrometric sphere and a structuring surface. Measurements were in fact performed with a cantilever where a sphere (r_1) was glued in place of the standard *AFM* tip, noted S_a . The size and the nature of the sphere were determined by the experimenter. The force calibration was performed for each cantilever with this resonance frequency and ten measurements were done at different locations on the same sample with a driving speed of 200 nm/s.

Spheres glued on the cantilever

All borosilicate spheres are provided by SPI Supplies and commercialized by Neyco (Paris, France). Diameters are certified using certified standards from the National Institute of Standards and Technology (*NIST*). The glassy carbon sphere, Sigradur K, is supplied by HTW (Germany). The power is spherical and the diameter is between 10 and 20 μm . Before experiment the carbon sphere gluing on the cantilever is measured in SEM. The glass spheres gluing has been performed in the laboratory with the Dymax 628-VLV glue and the Blue Wave 50 apparatus (Dymax, Garches, France). The glue was reticulated by UV light (365 nm).

Acknowledgement

This work was partially supported by the *EU* under *HYDROMEL* (contract NMP2-CT-2006-026622): Hybrid ultra precision manufacturing process based on positional- and self-assembly for complex

micro-products, and *FAB2ASM* (contract FoF-NMP-2010-260079): Efficient and Precise 3D Integration of Heterogeneous Microsystems from Fabrication to Assembly, and by the French National Agency (ANR) under *NANOROL* (contract ANR-07-ROBO-0003): Nanoanalyse for micromanipulate. We would also like to acknowledge the support of D. Rostoucher, *FEMTO-ST*, for sphere joining on the tipless extremity.

References

- (1) Tamadazte, B.; Dembélé, S.; Le Fort-Piat, N. A Multiscale Calibration of a Photon Videomicroscope for Visual Servo Control: Application to MEMS Micromanipulation and Microassembly. *Sens. Transducers J.* **2009**, *5*, 37–52.
- (2) Lambert, P. *Capillary Forces in Micro-assembly*; Springer: Amsterdam, The Netherlands, 2008.
- (3) Gauthier, M.; Régnier, S.; Rougeot, P.; Chaillet, N. Forces Analysis for Micromanipulations in Dry and Liquid Media. *J. Micromechatronics* **2006**, *3*, 389–413.
- (4) Zhou, Q.; Chang, B.; Koivo, H. N. Ambient Environment Effects in Micro/Nano handling. *Proceedings of the International Workshop on Microfactories*, Shanghai, China, oct. 15-17, 2004; IOP Publishing Ltd.: Bristol, U.K., 2004; pp 146–151.
- (5) Hériban, D.; Gauthier, M. Robotic Micro-Assembly of Microparts Using a Piezogripper. *Proceedings of the 2008 IEEE/RSJ International Conference on Intelligent Robots and Systems*, Nice, France, Sept 22-26, 2008; IEEE: Piscataway, NJ, 2008; pp 4042–4047.
- (6) Dafflon, M.; Lorent, B.; Clavel, R. A Micromanipulation Setup for Comparative Tests of Microgrippers. *International Symposium on Robotics (ISR)*, 2006.
- (7) Blomberg, E.; Poptoshev, E.; Claesson, P. M.; Caruso, F. Surface Interactions during Polyelectrolyte Multilayer Buildup. 1. Interactions and Layer Structure in Dilute Electrolyte solutions. *Langmuir* **2004**, *20*, 5432–5438.

- (8) Charrault, E.; Gauthier, C.; Marie, P.; Schirrer, R. Experimental and Theoretical Analysis of a Dynamic JKR Contact. *Langmuir* **2009**, *25*, 5847–5854.
- (9) Dejeu, J.; Rougeot, P.; Gauthier, M.; Boireau, W. Reduction of Micro-Object's using Chemical Functionalisation. *Micro Nano Lett.* **2009**, *4*, 74–79.
- (10) Wang, T.; Canetta, E.; Weerakkody, T. G.; Keddle, J. L. Nanomaterials: Sticky but not Messy. *ACS Appl. Mater. Interfaces* **2009**, *1*, 631–639.
- (11) Gong, H.; Garcia-Turiel, J.; Vasilev, K.; Vinogradova, O. I. Interaction and Adhesion Properties of Polyelectrolyte Multilayers. *Langmuir* **2005**, *21*, 7545–7550.
- (12) Rabenoroso, K.; Clevy, C.; Lutz, P.; Gauthier, M.; Rougeot, P. Evaluation of Pull-off Forces for Planar Contact in Micro-Assembly. *Micro Nano Lett.* **2009**, *4*, 148–154.
- (13) Vajpayee, S.; Hui, C.-Y.; Jagota, A. Model-Independent Extraction of Adhesion Energy from Indentation Experiments. *Langmuir* **2008**, *24*, 9401–9409.
- (14) Murphy, M. P.; Kim, S.; Sitti, M. Enhanced Adhesion by Gecko-Inspired Hierarchical Fibrillar Adhesives. *ACS Appl. Mater. Interfaces* **2009**, *1*, 849–855.
- (15) Johnson, K. L.; Kendall, K.; Roberts, A. D. Surface Energy and the Contact of Elastic Solids. *Proc. R. Soc. Lond. A, Ser. A* **1971**, *324*, 301–313.
- (16) Derjaguin, B. V.; Muller, V.; Toporov, Y. P. Effect of Contact Deformations on the Adhesion of Particles. *J. Colloid Interface Sci.* **1975**, *53*, 314–326.
- (17) Maugis, D. Adhesion of Spheres: the JKR-Transition Using a Dugdale Model. *J. Colloid Interface Sci.* **1992**, *150*, 243–269.
- (18) Jones, R.; Pollock, H. M.; Cleaver, J. A. S.; Hodges, C. S. Adhesion Forces between Glass and Silicon Surfaces in Air Studied by AFM: Effects of Relative Humidity, Particle Size, Roughness, and Surface Treatment. *Langmuir* **2002**, *18*, 8045–8055.

- (19) Hamaker, H. C. The London - van der Waals Attraction between Spherical Particules. *Physica* **1937**, *4*, 1058–1072.
- (20) Delrio, F. W.; de Boer, M.; Knapp, J.; Davidreedy, E.; Clews, P.; Dunn, M. The Role of van der Waals Forces in Adhesion of Micromachined Surfaces. *Nat. Mater.* **2005**, *4*, 629–634.
- (21) Alvo, S.; Lambert, P.; Gauthier, M.; Régnier, S. Adhesion Model for Micromanipulation Based on van der Waals Forces. *J. Adhes. Sci. Technol.* **2010**, *24*, 2415–2428.
- (22) Jaiswal, R. P.; Kumar, G.; Kilroy, C. M.; Beaudoin, S. P. Modeling and Validation of the van der Waals Force During the Adhesion of Nanoscale Objects to Rough Surfaces: a Detailed Description. *Langmuir* **2009**, *25*, 10612–10623.
- (23) Thoreson, E.; Martin, J.; Burnham, N. The Role of Few-Asperity Contacts in Adhesion. *J. Colloid Interface Sci.* **2006**, *298*, 94–101.
- (24) Li, Q.; Rudolph, V.; Peukert, W. London-van der Waals Adhesiveness of Rough Particles. *Powder Technol.* **2006**, *161*, 248–255.
- (25) Hodges, C. S.; Cleaver, J. A. S.; Ghadiri, M.; Jones, R.; Pollock, H. M. Forces between Polystyrene Particles in Water Using the AFM: Pull-Off Force vs Particle Size. *Langmuir* **2002**, *18*, 5741–5748.
- (26) Dejeu, J.; Bechelany, M.; Philippe, L.; Rougeot, P.; Michler, J.; Gauthier, M. Reducing the Adhesion between Surfaces Using Surface Structuration with PS Latex Particle. *ACS Appl. Mater. Interfaces* **2010**, *2*, 1630–1636.
- (27) Dejeu, J.; Rougeot, P.; Gauthier, M.; Boireau, W. Adhesions Forces Controlled by Chemical Self-Assembly and pH, Application to Robotic Microhandling. *ACS Appl. Mater. Interfaces* **2009**, *1*, 1966–1973.
- (28) Lupu, S.; Lakard, B.; Hihn, J.; Dejeu, J.; Rougeot, P.; Lallemand, S. Morphological Characterization and Analytical Application of Poly(3,4-ethylenedioxythiophene)-Prussian Blue

Composite Films Electrodeposited in situ on Platinum Electrode Chips. *Thin Solid Films* **accepted**.

- (29) Dejeu, J.; Taouil, A. E.; Rougeot, P.; Lakard, S.; Lallemand, F.; Lakard, B. Morphological and Adhesive Properties of Polypyrrole Films Synthesized by (Sono)Electrochemistry. *Synth. Met.* **2010**, *160*, 2540–2545.
- (30) Dejeu, J.; Rougeot, P.; Gauthier, M.; Boireau, W. Robotic Submerged Microhandling Controlled by pH Switching. *Proceedings of the IEEE IEEE/RSJ 2009 International Conference on Intelligent Robots and Systems*, St Louis, October 11-15, 2009.
- (31) Dejeu, J.; Rougeot, P.; Gauthier, M.; Boireau, W. Improvement of Robotic Micromanipulations Using Chemical Functionalizations. *IPAS 2010 (International Precision Assembly Seminar)*, *IFIP AICT 315*, 2010; pp 215–221.
- (32) Sausse Lhernould, M. S.; Delchambre, A.; Régnier, S.; Lambert, P. Electrostatic Forces in Micromanipulations: Review of Analytical Models and Simulations Including Roughness *Appl. Surf. Sci.* **2007**, *253*, 6203–6210.
- (33) Persson, B. N. J. Adhesion Between an Elastic Body and a Randomly Rough Hard Surface *Eur. Phys. J. E: Soft Matter Biol. Phys.* **2002**, *8*, 385–401.
- (34) Sahoo, P.; Chowdhury, S. K. R. A Fractal Analysis of Adhesive Wear at the Contact between Rough Solids *Wear* **2002**, *253*, 924–934.
- (35) Li, J.; Fu, J.; Cong, Y.; Wu, Y.; Xue, L. J.; Han, Y. C. Macroporous Fluoropolymeric Films Templated by Silica Colloidal Assembly, A Possible Route to Super-Hydrophobic Surfaces. *Appl. Surf. Sci.* **2006**, *252*, 2229–2234.
- (36) Kim, S. H.; Kim, J. H.; Kang, B. K.; Uhm, H. S. Superhydrophobic CF_x Coating via In-Line Atmospheric RF Plasma of He-CF₄-H₂. *Langmuir* **2005**, *21*, 12213–12217.

- (37) Han, J. T.; Zheng, Y.; Cho, J. H.; Xu, X.; Cho, K. Stable Superhydrophobic Organic-Inorganic Hybrid Films by Electrostatic Self-Assembly. *J. Phys. Chem. B* **2005**, *109*, 20773–20778.
- (38) Zhao, N.; Shi, F.; Wang, Z. Q.; Zhang, X. Combining Layer-by-Layer Assembly with Electrodeposition of Silver Aggregates for Fabricating Superhydrophobic Surfaces. *Langmuir* **2005**, *21*, 4713–4716.
- (39) Shi, F.; Wang, Z. Q.; Zhang, X. Combining a Layer-by-Layer Assembling Technique with Electrochemical Deposition of Gold Aggregates to Mimic the Legs of Water Striders. *Adv. Mater.* **2005**, *17*, 1005–1009.
- (40) Hikita, M.; Tanaka, K.; Nakamura, T.; Kajiyama, T.; Takahara, A. Super-Liquid-Repellent Surfaces Prepared by Colloidal Silica Nanoparticles Covered with Fluoroalkyl Groups. *Langmuir* **2005**, *21*, 7299–7302.
- (41) Jiang, L.; Zhao, Y.; Zhai, J. A Lotus-Leaf-like Superhydrophobic Surface: A Porous Microsphere/Nanofiber Composite Film Prepared by Electrohydrodynamics. *Angew. Chem., Int. Ed.* **2004**, *43*, 4338–4341.
- (42) Gu, Z. Z.; Wei, H. M.; Zhang, R. Q.; Han, G. Z.; Pan, C.; Zhang, H.; Tian, X. J.; Chen, Z. M. Artificial Silver Ragwort Surface. *Appl. Phys. Lett.* **2005**, *86*, 201915–201915–3.
- (43) Deckman, H.; Dunsmuir, J. Natural Lithography. *Appl. Phys. Lett.* **1982**, *41*, 377–379.
- (44) Sakamoto, S.; Philippe, L.; Bechelany, M.; Michler, J.; Asoh, H.; Ono, S. Ordered Hexagonal Array of Au Nanodots on Si Substrate Based on Colloidal Crystal Templating. *Nanotechnology* **2008**, *19*, 405304–405309.
- (45) Bechelany, M.; Brodard, P.; Philippe, L.; Michler, J. Extended Domains of Organized Nanorings of Silver Grains as Surface-Enhanced Raman Scattering Sensors for Molecular Detection. *Nanotechnology* **2009**, *20*, 455302–455309.

- (46) Bechelany, M.; Maeder, X.; Riesterer, J.; Hankache, J.; Lerose, D.; Christiansen, S.; Michler, J.; Philippe, L. Synthesis Mechanisms of Organized Gold Nanoparticles: Influence of Annealing Temperature and Atmosphere. *Cryst. Growth Des.* **2010**, 587–596.
- (47) Mook, W.; Niederberger, C.; Bechelany, M.; Philippe, L.; Michler, J. Compression of Free-standing Gold Nanostructures: from Stochastic Yield to Predictable Flow. *Nanotechnology* **2010**, 21, 55701.
- (48) Bechelany, M.; Brodard, P.; Elias, J.; Philippe, L.; Michler, J. Simple Synthetic Route for SERS Active Gold Nanoparticles Substrate with Controlled Shape and Organization. *Langmuir* **2010**, 26, 14364–14371.
- (49) Elias, J.; Lévy-Clément, C.; Bechelany, M.; Michler, J.; Wang, G.-Y.; Wang, Z.; Philippe, L. Hollow Urchin-like ZnO Thin Films by Electrochemical Deposition. *Adv. Mater.* **2010**, 22, 1607–1612.
- (50) Lerose, D.; Bechelany, M.; Philippe, L.; Michler, J.; Christiansen, S. Ordered Arrays of Epitaxial Silicon Nanowires Produced by Nanosphere Lithography and Chemical Vapor Deposition. *J. Cryst. Growth* **2010**, 312, 2887–2891.
- (51) Yoon, T.; Lee, H.; Yan, J.; Kim, D. Fabrication of SiC-Based Ceramic Microstructures from Preceramic Polymers with Sacrificial Templates and Lithographic Techniques-A Review. *J. Ceram. Soc. Jpn. Int. Ed.* **2006**, 114, 473–479.
- (52) Parfitt, G.; Picton, N. Stability of Dispersions of Graphitized Carbon Blacks in Aqueous Solutions of Sodium Dodecyl Sulphate. *Trans. Faraday Soc.* **1968**, 64, 1955–1964.
- (53) Agnus, J.; Hériban, D.; Gauthier, M.; Pétrini, V. Silicon End-Effectors for Microgripping Tasks. *Precis. Eng.* **2009**, 33, 542–548.